Estimating Stability and Resolution of Waveform Inversion Focal Mechanisms

S. Scolaro, C. Totaro, D. Presti, Sebastiano D'Amico, G. Neri and B. Orecchio

1 Introduction

The main aim of this study is to describe several tools for testing the stability and resolution of waveform inversion focal mechanisms already successfully adopted for crustal earthquakes occurred in the Calabrian Arc region, southern Italy (Fig. 1). It is well known that focal mechanism quality can decrease for low magnitude earthquakes and that, on overall, several factors can influence the results of seismic waveform inversion, for example seismic network coverage, earth model uncertainties and inaccurate earthquake location (Valentine and Trampert 2012; Chen et al. 2013; Brandmayr et al. 2013; Silwal and Tape 2016). Earthquake focal mechanisms can be considered as a primary tool for studying the interactions between earthquakes, seismic faults, and active tectonics (Anderson et al. 1993). Information coming from focal mechanisms is unfortunately confined to the time period of instrumental record-

S. Scolaro · C. Totaro · D. Presti · G. Neri · B. Orecchio
Department of Mathematics, Computer Sciences, Physics, and Earth Sciences, University of Messina, Viale F. Stagno D'Alcontres, 31, 98166 Messina, Italy
e-mail: silscolaro@unime.it

C. Totaro
e-mail: ctotaro@unime.it

D. Presti
e-mail: dpresti@unime.it

G. Neri
e-mail: geoforum@unime.it

B. Orecchio
e-mail: orecchio@unime.it

S. D'Amico (✉)
Department of Geosciences, University of Malta, Msida MSD 2080, Malta
e-mail: sebastiano.damico@um.edu.mt

S. D'Amico (ed.), *Moment Tensor Solutions*, Springer Natural Hazards,
https://doi.org/10.1007/978-3-319-77359-9_5

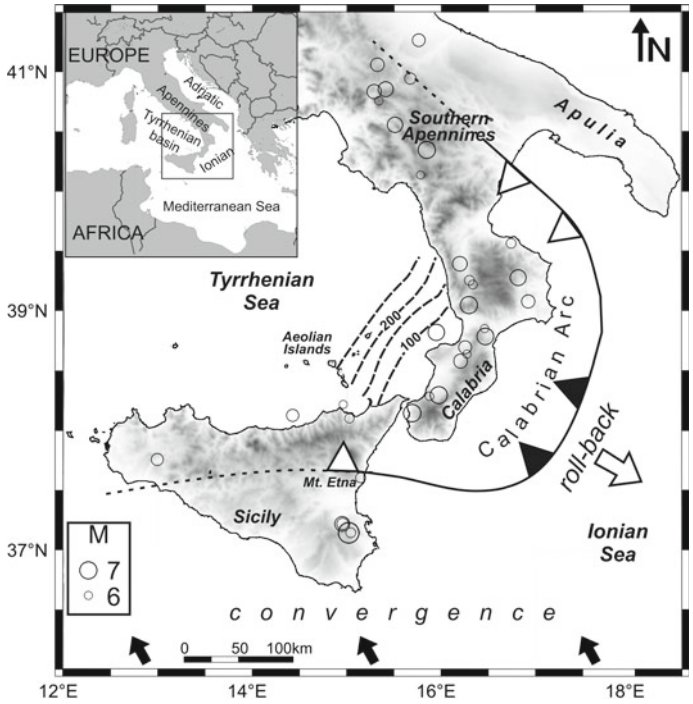

Fig. 1 Map view of southern Italy. The solid curve with the sawtooth pattern indicates the present-day location of the Ionian subducting system. According to recent literature, black sawteeth indicate the continuous subducting slab while white sawteeth the plate boundary segments where slab has already undergone detachment (see, among others, Neri et al. 2009, 2012; Orecchio et al. 2014). The white arrow shows the sense of the subducting slab rollback. The black arrows indicate the present motion of Africa relative to Europe (Nocquet 2012 and references therein). Circles show the locations of the earthquakes of magnitude 6.0 and larger that have occurred after 1000 A.D. according to the CPTI15 catalog (Rovida et al. 2016; http://emidius.mi.ingv.it/CPTI15). Thick dashed lines are depth contour lines of the Wadati-Benioff zone (Faccenna et al. 2011). In the upper right inset we report the study area (black box) in the wider regional framework

ings and processing of the historical seismograms (i.e. early XX century seismograph recordings) is often difficult (Batlló et al. 2008; Palombo and Pino 2013). Reliable source information is generally available for earthquakes of $M \geq 5.5$ that occurred after the inception of the World-Wide Standardized Seismic Network (WWSSN) in the early 1960s.

The methods traditionally used to compute focal mechanism solutions are based on the polarity of P-wave first motion. First-motion focal solutions reflect only the initial stages of faulting and strongly suffer from both uncertainty on velocity models used to reconstruct the wave path and inadequate azimuthal coverage of seismic

networks (Lay and Wallace 1995; Pondrelli et al. 2006; Scognamiglio et al. 2009; D'Amico et al. 2010; Presti et al. 2013). Moreover, errors in first-motion observations may occur because of station polarity reversals or incorrect direct P-arrival picks due to low signal-to-noise ratio. Much more powerful methods capable to furnish more stable and reliable focal mechanisms with respect to the traditional techniques are those based on waveform inversion (e.g. CMT, RCMT, TDMT). The Harvard Centroid Moment Tensor database (CMT; http://www.globalcmt.org) provides robust and reliable seismic source mechanisms through the inversion of long period (T > 45 s) body-waves and very-long period (T > 132 s) surface waves recorded at the global scale for earthquakes occurred since 1976 with $M_w > 4.5$ (Ekström et al. 2012). The European-Mediterranean Centroid Moment Tensor (RCMT; http://www.bo.ingv.it/RCMT/) procedure is based on the inversion of intermediate and long period surface waves recorded at regional and teleseismic distances (Pondrelli et al. 2002, 2004, 2006, 2007, 2011). The Time Domain Moment Tensor (TDMT; http://earthquake.rm.ingv.it/tdmt.php) algorithm performs long-period full waveform inversion for local and regional events with magnitude $M_w \geq 3.5$ (Dreger 2003; Dreger and Helmberger 1993; Scognamiglio et al., 2009).

During the last years, our research team made continuous processing and improvements on Calabrian Arc earthquake focal mechanisms in order to increase their reliability and to expand the temporal and magnitude range of focal mechanism databases (Neri et al. 2003, 2004, 2005; D'Amico et al. 2010, 2011, 2013; Presti et al. 2013; Totaro et al. 2013, 2015, 2016). We provided in Totaro et al. (2016) the most updated database including 438 crustal earthquake focal mechanisms for southern Italy (Fig. 2). Most of these focal mechanisms (344) have been computed by using the waveform inversion method Cut and Paste (CAP, Zhao and Helmberger 1994; Zhu and Helmberger 1996). This method have shown to furnish reliable and high-quality focal mechanism solutions also for relatively low-magnitude earthquakes (down to a minimum of ca. 2.6) not reported in the national catalogues and often not well resolved by using P-wave first motions (D'Amico et al. 2010, 2011). Because of their frequent occurrence, these small earthquakes are particularly important for characterizing local tectonics and constraining stress orientations.

The Calabrian Arc (Fig. 1) is the result of the convergence between Africa and Europe in the central Mediterranean (Billi et al. 2011; Faccenna et al. 2004; Rosenbaum and Lister 2004). This area is characterized by very heterogeneous seismotectonic regimes along its length (Cristofolini et al. 1985; Montone et al. 2004; Totaro et al. 2016) and has been the site of destructive earthquakes (M > 6) that occurred both in recent and historical times (Galli et al. 2008; Neri et al. 2006). The tectonic framework of the Calabrian Arc is complicated by the presence of a narrow subducting slab beneath Calabria (Neri et al. 2009; Orecchio et al. 2014 Selvaggi and Chiarabba 1995) and of two active volcanic districts: the Mt Etna in eastern Sicily and Aeolian Islands in southeastern Tyrrhenian (Carminati et al. 2010; Peccerillo 2003). In the study area, different lithospheric units with changing thickness, composition and velocity have been detected, even if the exact location of their boundaries, together with the effective role of slow-rate Africa-Eurasia convergence and residual Ionian slab rollback on regional geodynamics are still matter of debate (Carafa et al. 2015;

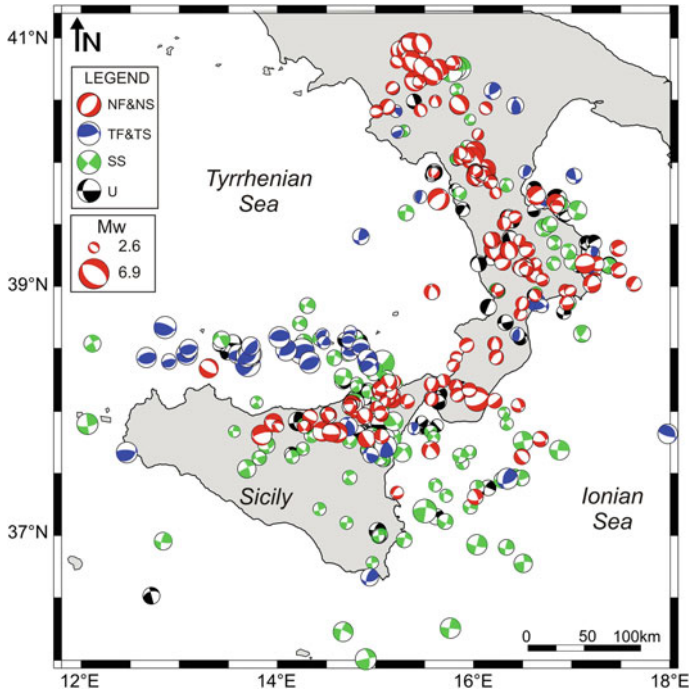

Fig. 2 Crustal earthquake focal mechanism catalogue for the study area. Different colors identify different types of mechanisms following Zoback's (1992) classification based on values of plunges of P and T axes: red = normal faulting (NF) or normal faulting with a minor strike-slip component (NS); green = strike-slip faulting (SS); blue = thrust faulting (TF) or thrust faulting with a minor strike-slip component (TS); black = unknown stress regime (U). "U" includes all focal mechanisms which do not fall in the other five categories (Zoback 1992). The beach ball size is proportional to the earthquake magnitude (see legend)

Faccenna et al. 2014; Gallais et al. 2013; Peròuse et al. 2012; Devoti et al. 2008). Well constrained focal mechanisms obtained in the last years provide a key element to study the regional tectonic processes in the Calabrian Arc region characterized by high heterogeneity in terms of seismotectonics and kinematics.

2 Data

Since it is widely accepted that waveform inversion focal solutions in the study area are much better constrained than P onset polarity ones (see, among others, Presti et al. 2013; Scognamiglio et al. 2009; Pondrelli et al. 2006), all the focal mecha-

nisms selected in the present work are waveform inversion solutions (i) computed by the CAP method or (ii) coming from Italian centroid moment tensor (ItCMT, i.e. Centroid Moment Tensors computed from the Italian region http://rcmt2.bo.ingv.it/Italydataset.html), and (iii) time domain moment tensor (TDMT) catalogs (http://cnt.rm.ingv.it/tdmt). In particular, our database (Fig. 2) consists of 438 waveform inversion focal mechanisms coming from catalogues (104 solutions) and computed by the CAP method (334 solutions). Concerning the data coming from catalogues, most of them are from the Italian CMT catalog (time interval 1976-present, $M_w \geq 4$; Pondrelli et al. 2006) obtained by merging the existing global CMTs and European-Mediterranean RCMTs data for the Italian region. For the period 2006–2015 the database also includes focal solutions computed by using the Time-Domain Moment Tensor ($M_w \geq 3.5$). The CAP focal mechanisms have been estimated for earthquakes of magnitude $M_w \geq 2.6$ that originated at depths shallower than 40 km in the study region between January 2006 and October 2015. The CAP method allows to compute reliable and high-quality focal mechanism solutions also for relatively low-magnitude earthquakes ($2.6 \leq M_w \leq 3.5$) usually not reported in the national catalogues and often not well resolved by using P-wave first motions (D'Amico et al. 2010, 2011; Orecchio et al. 2015; Totaro et al. 2016). Thus, it permitted to strongly increase the amount of data available for the southern Italy region. Since the 90% of our dataset is composed by focal mechanisms computed by applying the CAP method, we carried out several analyses aiming to evaluate stability and resolution of the algorithm. In addition, we also performed different tests in order to estimate error on focal mechanism parameters.

3 The CAP Inversion Method

In the CAP method (Zhao and Helmberger 1994, 1996), each waveform is broken up into P_{nl} (P_n followed by train of crust-trapped reflected/converted P-SV) and surface wave segments, which are weighted differently during the inversion procedure. The use of different portion of the waveform increases the stability of the final solution since different phases are sensitive to different parts of crustal structure and have different amplitude decay with distances. The surface waves, although large in amplitudes, are easily influenced by shallow crustal heterogeneities whereas P_{nl} waves are controlled by the averaged crustal velocity structure and are therefore more stable.

In order to invert the data, waveforms are converted in ground velocity and preferred to ground displacement mainly because the majority of the events have magnitude smaller than four and we needed to avoid the influence of long-period noise embedded in ground displacements. Furthermore, working with ground velocity rather than ground displacement reduces the influence of a low frequency site or instrument noise on the deconvolution. The same frequency bands have been used to filter synthetic and observed ground velocities, in detail 0.02–0.1 Hz for surface waves and 0.05–0.3 Hz for P_{nl} waves. All these features make the CAP method

effective for earthquakes over a wide range of magnitudes (down to a minimum of 2.6; D'Amico et al. 2010, 2011; Zhu et al. 2006) as also proven by several tests and comparisons (D'Amico et al. 2010, 2011; Tan et al. 2006; Zhao and Helmberger 1994; Totaro et al. 2016).

4 Stability Tests and Resolution Estimates

The use of CAP in the Calabrian Arc region has allowed to estimate focal mechanism solutions also for low magnitude events (down to a minimum of 2.6) and therefore to significantly increase the number of focal mechanisms based on waveform inversion method (i.e., 90% of the dataset comes from CAP inversions). Such a relevant increase has important implications for better constrain local stress conditions and geodynamic interpretations in the study area (Totaro et al. 2016 and references therein). Hence it is necessary to carefully check quality and stability of newly-added waveform inversion solutions estimated by CAP method. Starting from these considerations and by also taking into account concerned literature information (see e.g., D'Amico et al. 2010, 2011; Presti et al. 2013; Orecchio et al. 2014) we present in this study several resolution and stability tests aimed to properly verify the robustness of CAP results.

We report the results of several tests performed on a subset of 5 earthquakes chosen as representative of different network condition, magnitude value, location area and focal depth.

For each earthquake we observed how the moment tensor varies as function of focal depth in order to evaluate its stability around the global misfit minimum. The depth increment in the grid search is 5 km and for each depth we report the best-fit solution obtained by searching over the full space of orientations and magnitudes and the relative misfit value.

Then, we repeated the inversion procedure by considering different seismic network distribution. Seismic network geometry is fundamental in the earthquake analysis. In particular, in our study region the network configuration is often limited by the presence of wide off-shore sectors and the substantial lack of OBS (Ocean Bottom Seismometer) data. This factor can reduce the quality of solutions and therefore we verify CAP results even with not-optimal azimuthal coverage and few available records by using earthquake located both on-shore and off-shore in the Calabrian Arc area.

Also, we investigated the influence of epicentral errors on the waveform inversion. Non-linear earthquake locations performed in the study area using the method by Presti et al. (2004, 2008) and consequent hypocentral error evaluation indicate that the mean epicentral uncertainty is in the range of 4–6 km (Orecchio et al. 2014). Then we forced the epicenter to lie 5 km away from the true location in order to test the solution even taking into account the mean uncertainty on earthquake location.

An important role in waveform inversion procedure is also played by the seismic velocity model that is used for the calculation of Green's Functions basically for

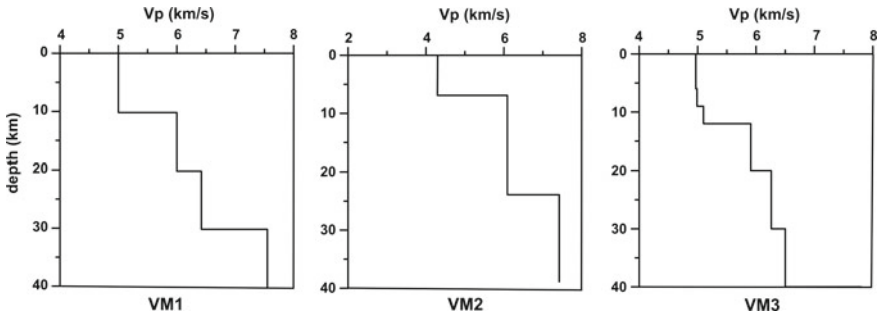

Fig. 3 Different velocity models used to compute the Green's functions for tests on the influence of possible crustal structure heterogeneities in the study area (see also plot c in Fig. 4)

the double-couple mechanism estimates. Each focal mechanism of the most updated CAP catalog (Totaro et al. 2016) has been computed by using a specific 1D velocity model for each target area. To take into account the lithospheric heterogeneities of the Calabrian Arc region we used the most detailed 3D velocity models available from the literature (Barberi et al. 2004; Orecchio et al. 2011; Totaro et al. 2014) to compute theoretical travel times for properly defined target area and to build from these specific 1D velocity models (D'Amico et al. 2011). Even if the time-shift allowed in the CAP algorithm can partly reduce the influence introduced by the velocity model uncertainties, we further verified the stability of the solution with respect to velocity structure by using different velocity models representative of structure heterogeneities of the study region (Fig. 3).

Generally, waveform inversion methods give a standard error for each focal mechanism parameter (e.g., strike, dip and rake) derived from linearized techniques. It provides an important and useful measure of quality of focal mechanism solution but, as shown by several authors, linearized inversion methods tend to underestimate formal errors on focal mechanism parameter (Tan et al. 2006; Bevington and Robinson 2003). We present a procedure aimed to assess more reliable confidence limits of estimated strike, dip and rake. Following the approach described by Stich et al. (2003), we used a grid search for error analysis in the full range of focal parameter space. For each earthquake a set of "artificial" focal mechanisms has been obtained by moving around the best-fit solution in all directions of the focal parameter space with a sampling step of 10°. Then we estimated the misfit for all artificial focal mechanisms and compared these values with the global minimum misfit of the best solution obtained by CAP. In this way it is possible to observe how the misfit value changes with respect to strike, dip and rake, respectively. This comparison can assess the confidence limits and the range of potential alternative solutions over fault plane parameters, allowing us to define the accuracy of the focal mechanism solution. According to Stich et al. (2003), we assumed that the uncertainty region of the solution includes all the artificial focal mechanisms having misfit <10% above the global minimum. By application of this procedure to CAP moment tensor solutions

Table 1 Events used in th study

ID event	DATE yy/mm/dd	TIME hh:mm:ss	Lat (°)	Lon (°)	Depth (km)	Strike	Dip	Rake	M_w
1	20090701	17:58:54	38.34	15.01	2	40	90	19	3.1
2	20111119	10:19:16	16.00	37.81	14	121	70	−25	3.4
3	20140323	18:31:52	37.47	16.48	38	177	61	21	3.6
4	20140708	05:02:43	39.90	16.12	2	347	51	−83	2.9
5	20150329	10:48:46	38.09	16.21	12	52	76	−83	3.5

we are able to estimate that our focal mechanism solutions are characterized by fault parameter errors of the order of 8°–10° (Totaro et al. 2016).

5 Results and Discussion

In Fig. 4 we report the results of the above described tests performed for the 5 events listed in Table 1 and chosen to fairly represent dataset heterogeneities. For each event the epicenter location (black star) and the recording seismic network (triangles) are shown on plots (a). The earthquakes are located both on-shore and off-shore (ID 2, 4 and 1, 3, 5 in Fig. 4, respectively) in the Calabrian Arc area and they are also characterized by different network coverage. We display on plots (b) the best focal mechanism solution in the waveform misfit versus depth curve obtained by the grid search procedure. From plot (b) we can observe that, in general, the focal solution does not change significantly near the minimum misfit value. Only for the earthquake ID 3, located in the Ionian Sea, the curve of waveform misfit is almost flat around the minimum indicating that the network coverage does not provide a tight depth constraint.

As already mentioned, we assess inversion results also by using different station configurations as indicated in the left column of plots (c) of Fig. 4 where we also report the respective best focal mechanism solution. In all cases the focal mechanisms are very similar to that obtained from the inversion with the real station network. Even in this case some differences between the focal mechanisms calculated by test and the true one are visible for earthquake ID 3 and may be probably related to the position of the epicenter with respect to the recording stations. By also taking into account these small differences this test shows the good stability of CAP results even in case of poor station distribution or quite low magnitude. By way of example see, events ID 3, ID 4, and ID 5: for these earthquakes, in fact, the seismic network configuration has an azimuthal gap as large as 180° and also the simulation in extremely bad conditions characterized by only 2 recording stations show very stable solutions. Plots (c) of Fig. 4 also report (right side) the focal mechanisms obtained by varying of 5 km the epicenter location (grey star in plots a). It clearly appears that a mislocation compatible with the hypocenter location uncertainties estimated does not produce

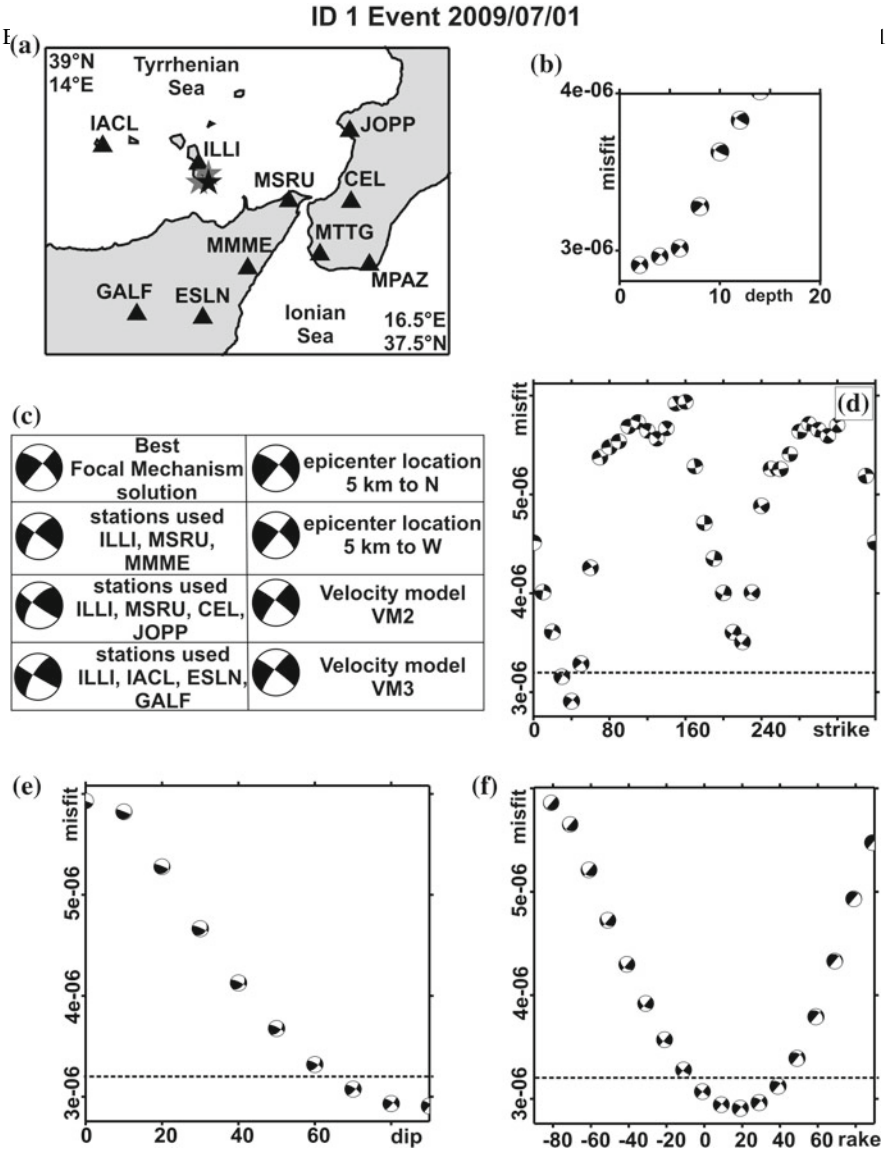

Fig. 4 The figure shows results obtained after tests performed to verify the stability and the error on CAP focal mechanism solutions. Plot **a** map reporting recording stations (black triangles) and epicentral location (black star) used in the waveform inversion procedure together with two biased epicentral locations used for synthetic tests (grey stars) for each event. Plot **b** misfit error as function of depth. Plot **c** reports the best focal mechanisms solution for each earthquake and the results of different tests performed by changing the recording networks (also using very unfavourable conditions), the velocity models for the study area (see Fig. 3) and by forcing the epicenters to lie 5 km away from the "true" locations. Plots **d**, **e**, **f** reports the graph of RMS versus strike, dip and rake, respectively. The dashed line marks the 10% threshold of RMS. The minimum shown in each diagram is the best solution of the event

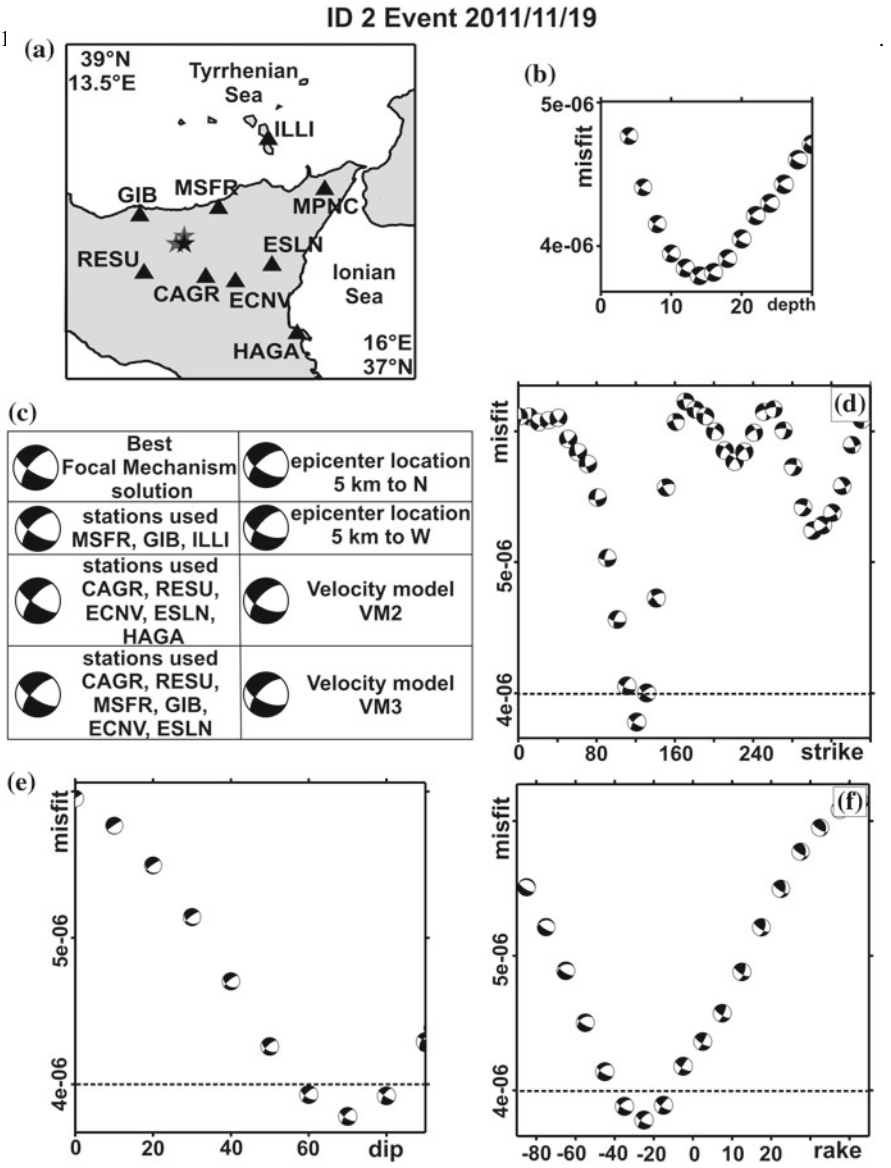

Fig. 4 (continued)

significant differences between true and simulated solution, further supporting the stability of our results. In the same plots we compare the solutions estimated using different 1D velocity models, VM1, VM2 and VM3 (Fig. 3), used for computation of the focal mechanisms. Even in these examples, the high stability of the mechanisms is evident. More pronounced differences affect the results of event ID 3, probably due to inaccuracy of the model VM2 and VM3 for the Ionian Sea area. Plots (d), (e) and (f) of Fig. 4 report the misfit values versus strike, dip and rake respectively. These

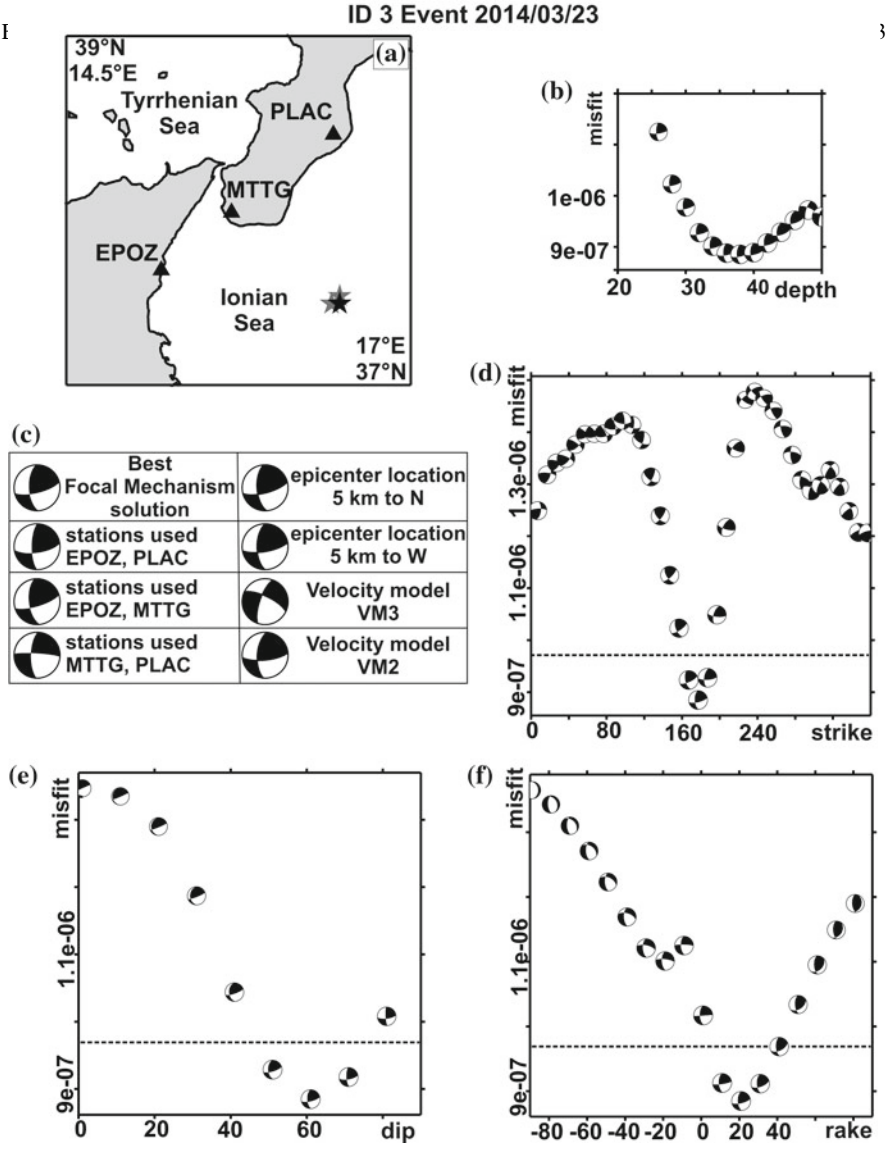

Fig. 4 (continued)

diagrams useful to study the uncertainties of the focal mechanism solution have been built by estimating the misfit values throughout the space of moment tensor orientations. As the uncertainly volume is defined by misfit lower than 10° respect to the best moment tensor solution all the focal mechanisms under the dashed line are acceptable solutions. Usually, relying on focal mechanisms that follow the 10% threshold we can estimate that our focal parameter errors are on average of 8°–10°, like in the examples here reported.

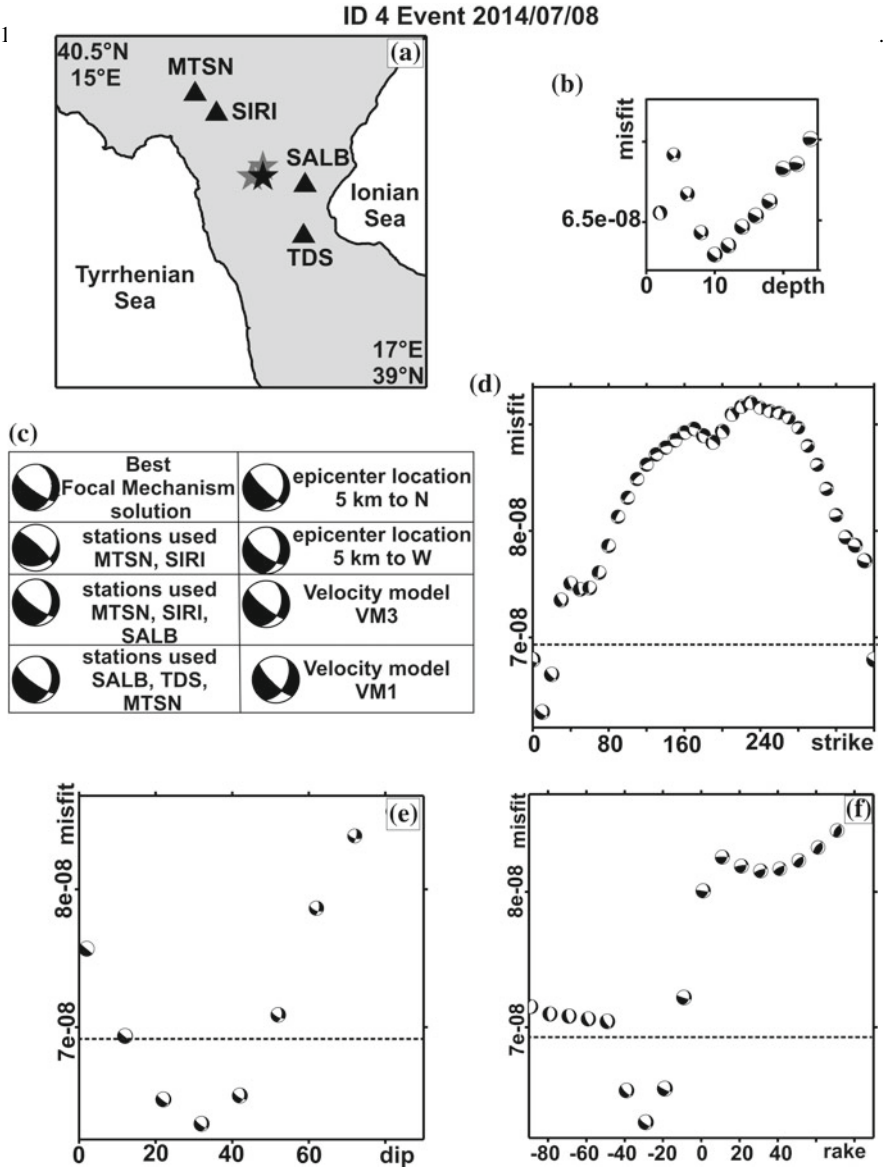

Fig. 4 (continued)

6 Concluding Remarks

In order to check the method robustness, the quality and stability of CAP focal mechanism solutions have been proven by mean of several tests also for low magnitude earthquakes. Following previous investigations carried out in the study region, we performed tests taking into account (1) recording station geometry, (2) different

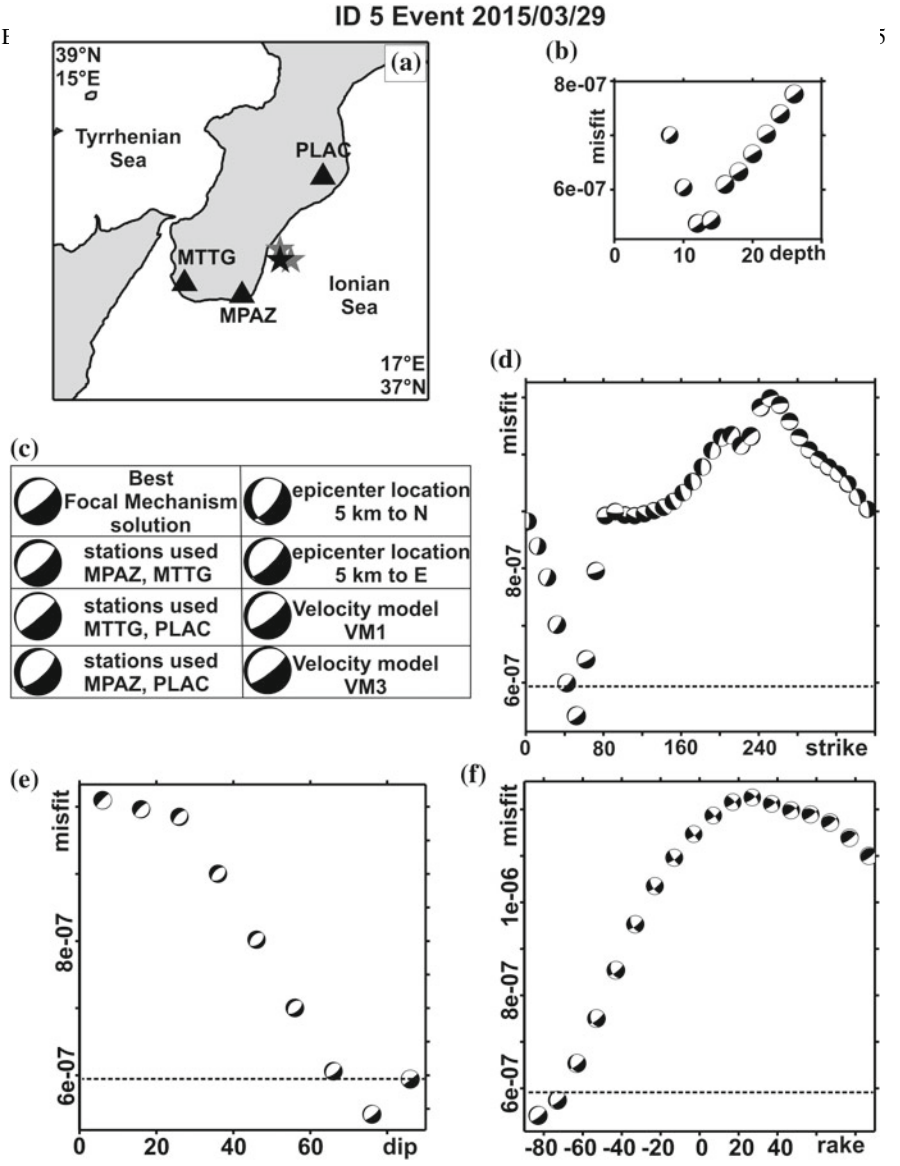

Fig. 4 (continued)

velocity models, (3) the misfit error as a function of depth, (4) epicenter uncertainty, and (5) strike, dip and rake variations as function of waveform misfit. Through these tests we verified that CAP solutions are robustly determined and just a few stations provide enough information to properly constrain the earthquake focal mechanism. Furthermore, the application of CAP method can provide good-quality solutions in a magnitude range (i.e. $2.6 \leq M_w \leq 3.5$) not properly represented in the Italian national

catalogues and where the solutions estimated from P-onset polarities are often poorly constrained.

The procedures described in this paper could be applied to different datasets in order to verify the robustness of estimated focal mechanisms and, consequently, to properly improve the knowledge of the seismotectonic regime, regional stress field features as well as the seismic hazard of different investigation areas.

Acknowledgements Some Figures were created using the Generic Mapping Tools (GMT) by Wessel and Smith (1991).

References

Anderson H, Webb T, Jackson J (1993) Focal mechanisms of large earthquakes in the south-island of New Zealand—implications for the accommodation of Pacific-Australia plate motion. Geophys J Int 115:1032–1054. https://doi.org/10.1111/j.1365-246X.1993.tb01508.x

Barberi G, Cosentino MT, Gervasi A, Guerra I, Neri G, Orecchio B (2004) Crustal seismic tomography in the Calabrian Arc region, south Italy. Phys Earth Planet Inter 147:297–314

Batlló J, Stich D, Macià R (2008) Quantitative analysis of early seismograph recordings. In: Historical seismology. Springer, Dordrecht, pp 385–402

Bevington PR, Robinson DK (2003) Data Reduction and error analysis. McGraw-Hill, New York

Billi A, Faccenna C, Bellier O, Minelli L, Neri G, Piromallo C, Presti D, Scrocca D, Serpelloni E (2011) Recent tectonic reorganization of the Nubia-Eurasia convergent boundary heading for the closure of the western Mediterranean. Bull de la Société Géologique de Fr 182(4):279–303

Brandmayr E, Romanelli F, Panza GF (2013) Stability of fault plane solutions for the major N Italy seismic events in 2012. Tectonophysics 608:525–529

Carafa M, Barba S, Bird P (2015) Neotectonics and long-term seismicity in Europe and the Mediterranean region. J Geophys Res Solid Earth 120(7):5311–5342

Carminati E, Lustrino M, Cuffaro M, Doglioni C (2010) Tectonics, magmatism and geodynamics of Italy: what we know and what we imagine. J Virtual Explorer 36. http://dx.doi.org/10.3809/jvirtex.2010.00226

Chen W, Wang D, Wei S (2013) A study on the uncertainties of the centroid depth of the 2013 Lushan earthquake from teleseimic body wave data. Earthq Sci 26(3–4):161–168

Cristofolini R, Ghisetti F, Scarpa R, Vezzani L (1985) Character of the stress field in the Calabrian arc and southern Apennines (Italy) as deduced by geological, seismological and volcanological information. Tectonophysics 117(1):39–58

D'Amico S, Orecchio B, Presti D, Zhu L, Herrmann RB, Neri G (2010) Broadband waveform inversion of moderate earthquakes in the Messina Straits, southern Italy. Phys Earth Planet Inter 179(3–4):97–106

D'Amico S, Orecchio B, Presti D, Gervasi A, Zhu L, Guerra I, Neri G, Herrmann RB (2011) Testing the stability of moment tensor solutions for small earthquakes in the Calabro-Peloritan Arc region (southern Italy). Bollettino di Geofisica Teorica ed Applicata 52(2):283–298

D'Amico S, Lombardo G, Panzera F (2013) Seismicity of the Mediterranean region and mitigation of earthquake losses. Phys Chem Earth 63:1–2. https://doi.org/10.1016/j.pce.2013.07.001

Devoti R, Riguzzi F, Cuffaro M, Doglioni C (2008) New GPS constraints on the kinematics of the Apennines subduction, Earth Planet. Sci Lett 273:163–174

Dreger DS, Helmberger DV (1993) Determination of source parameters at regional distances with three-component sparse network data. J Geophys Res Solid Earth 98(B5):8107–8125

Dreger D (2003) TDMT_INV: time domain seismic moment tensor INVersion. In: International handbook of earthquake and engineering seismology, vol 81B, p 1627

Ekström G, Nettles M, Dziewonski AM (2012) The global CMT project 2004–2010: Centroid-moment tensors for 13,017 earthquakes. Phys Earth Planet Inter 200–201. https://doi.org/10.1016/j.pepi.2012.04.002

Faccenna C, Piromallo C, Crespo-Blanc A, Jolivet L, Rossetti F (2004) Lateral slab deformation and the origin of the western Mediterranean arcs. Tectonics 23(1)

Faccenna C, Molin P, Orecchio B, Olivetti V, Bellier O, Funiciello F, Minelli L, Piromallo C, Billi A (2011) Topography of the Calabria subduction zone (southern Italy): clues for the origin of Mt Etna. Tectonics 30, TC1003. http://dx.doi.org/10.1029/2010TC002694

Faccenna C, Becker TW, Auer L, Billi A, Boschi L, Brun JP, Capitanio FA, Funiciello F, Horvàth F, Jolivet L, Piromallo C, Royden L, Rossetti F, Serpelloni E (2014) Mantle dynamics in the Mediterranean. Rev Geophys 52(3):283–332

Gallais F, Graindorge D, Gutscher MA, Klaeschen D (2013) Propagation of a lithospheric tear fault (STEP) through the western boundary of the Calabrian accretionary wedge offshore eastern Sicily (Southern Italy). Tectonophysics 602:141–152

Galli P, Galadini F, Pantosti D (2008) Twenty years of paleoseismology in Italy. Earth Sci. Rev. 88:89–117

Lay T, Wallace TC (1995) Modern global seismology, vol 58. Academic press

Montone P, Mariucci MT, Pondrelli S, Amato A (2004) An improved stress map for Italy and surrounding regions (central Mediterranean). J Geophys Res Solid Earth 109(B10)

Neri G, Barberi G, Orecchio B, Mostaccio A (2003) Seismic strain and seismogenic stress regimes in the crust of the southern Tyrrhenian region. Earth and Planet Sci Lett 213(1):97–112

Neri G, Barberi G, Oliva G, Orecchio B (2004) Tectonic stress and seismogenic faulting in the area of the 1908 Messina earthquake, south Italy. Geophys Res lett 31(10)

Neri G, Barberi G, Oliva G, Orecchio B (2005) Spatial variations of seismogenic stress orientations in Sicily, south Italy. Phys Earth Planet Inter 148(2):175–191

Neri G, Oliva G, Orecchio B, Presti D (2006) A possible seismic gap within a highly seismogenic belt crossing Calabria and eastern Sicily, Italy. Bull Seismol Soc Am 96(4A):1321–1331

Neri G, Orecchio B, Totaro C, Falcone G, Presti D (2009) Subduction beneath southern Italy close the ending: Results from seismic tomography. Seismol Res Lett 80(1):63–70

Neri G, Marotta AM, Orecchio B, Presti D, Totaro C, Barzaghi R, Borghi A (2012) How lithospheric subduction changes along the Calabrian arc in southern Italy: Geophysical evidences. Int J Earth Sci 101(7):1949–1969. https://doi.org/10.1007/s00531-012-0762-7

Nocquet JM (2012) Present-day kinematics of the Mediterranean: a comprehensive overview of GPS results. Tectonophysics 579:220–242. https://doi.org/10.1016/j.tecto.2012.03.037

Orecchio B, Presti D, Totaro C, Guerra I, Neri G (2011) Imaging the velocity structure of the Calabrian Arc region (South Italy) through the integration of different seismological data. Bollettino di Geofisica Teorica ed Applicata 52:625–638

Orecchio B, Presti D, Totaro C, Neri G (2014) What earthquakes say concerning residual subduction and STEP dynamics in the Calabrian Arc region, south Italy. Geophys J Int 199(3):1929–1942

Orecchio B, Presti D, Totaro C, D'Amico S, Neri G (2015) Investigating slab edge kinematics through seismological data: The northern boundary of the Ionian subduction system (south Italy). J Geodyn 88:23–35

Palombo B, Pino NA (2013) On the recovery and analysis of historical seismograms. Ann Geophys 56(3):0326

Peccerillo A (2003) Plio-quaternary magmatism in Italy. Episodes 26:222–226

Perouse E, Chamot-Rooke N, Rabaute A, Briole P, Jouanne F, Georgiev I, Dimitrov D (2012) Bridging onshore and offshore present-day kinematics of central and eastern Mediterranean: implications for crustal dynamics and mantle flow. Geochem Geophys Geosyst 13(9)

Pondrelli S, Morelli A, Ekström G, Mazza S, Boschi E, Dziewonski AM (2002) European-Mediterranean regional centroid-moment tensors: 1997–2000. Phys Earth Planet Inter 130(1):71–101

Pondrelli S, Morelli A, Ekstrom G (2004) European-Mediterranean regional centroid-moment tensor catalog: solutions for years 2001 and 2002. Phys Earth Planet Inter 145(1–4):127–147

Pondrelli S, Salimbeni S, Ekström G, Morelli A, Gasperini P, Vannucci G (2006) The Italian CMT dataset from 1977 to the present. Phys Earth Planet Inter 159(3):286–303
Pondrelli S, Salimbeni S, Morelli A, Ekström G, Boschi E (2007) European-Mediterranean regional centroid moment tensor catalog: solutions for years 2003 and 2004. Phys Earth Planet Inter 164(1):90–112
Pondrelli S, Salimbeni S, Morelli A, Ekström G, Postpischl L, Vannucci G, Boschi E (2011) European-Mediterranean regional centroid moment tensor catalog: solutions for 2005–2008. Phys Earth Planet Inter 185(3):74–81
Presti D, Troise C, De Natale G (2004) Probabilistic location of seismic sequences in heterogeneous media. Bull Seismol Soc Am 94(6):2239–2253
Presti D, Orecchio B, Falcone G, Neri G (2008) Linear versus non-linear earthquake location and seismogenic fault detection in the southern Tyrrhenian Sea, Italy. Geophys J Int 172:607–618
Presti D, Billi A, Orecchio B, Totaro C, Faccenna C, Neri G (2013) Earthquake focal mechanisms, seismogenic stress, and seismotectonics of the Calabrian Arc, Italy. Tectonophysics 602:153–175
Rosenbaum G, Lister GS (2004) Neogene and Quaternary rollback evolution of the Tyrrhenian Sea, the Apennines, and the Sicilian Maghrebides. Tectonics 23(1)
Rovida A, Locati M, Camassi R, Lolli B, Gasperini P (2016) CPTI15, the 2015 version of the Parametric Catalogue of Italian Earthquakes, Istituto Nazionale di Geofisica e Vulcanologia. http://emidius.mi.ingv.it/CPTI/, https://doi.org/10.6092/ingv.it-cpti15
Selvaggi G, Chiarabba C (1995) Seismicity and P-wave velocity image of the southern Tyrrhenian subduction zone. Geophys J Int 121(3):818–826
Scognamiglio L, Tinti E, Michelini A (2009) Real-time determination of seismic moment tensor for the Italian region. Bull Seismol Soc Am 99(4):2223–2242
Silwal V, Tape C (2016) Seismic moment tensors and estimated uncertainties in southern Alaska. J Geophys Res Solid Earth 121(4):2772–2797
Stich D, Ammon CJ, Morales J (2003) Moment tensor solutions for small and moderate earthquakes in the Ibero—Maghreb region. J Geophys Res Solid Earth 108(B3)
Tan Y, Zhu L, Helmberger D, Saikia C (2006) Locating and modeling regional earthquakes with two stations. J Geophys Res 111:B01306
Totaro C, Presti D, Billi A, Gervasi A, Orecchio B, Guerra I, Neri G (2013) The ongoing seismic sequence at the Pollino Mountains, Italy. Seismol Res Lett 84(6):955–962
Totaro C, Koulakov I, Orecchio B, Presti D (2014) Detailed crustal structure in the area of the southern Apennines-Calabrian Arc border from local earthquake tomography. J Geodyn 82:87–97
Totaro C, Seeber L, Waldhauser F, Steckler M, Gervasi A, Guerra I, Orecchio B, Presti D (2015) An intense earthquake swarm in the southernmost Apennines: fault architecture from high-resolution hypocenters and focal mechanisms. Bull Seismol Soc Am
Totaro C, Orecchio B, Presti D, Scolaro S, Neri G (2016) Seismogenic stress field estimation in the Calabrian Arc region (south Italy) from a Bayesian approach. Geophys Res Lett 43(17):8960–8969
Valentine AP, Trampert J (2012) Assessing the uncertainties on seismic source parameters: towards realistic error estimates for centroid-moment-tensor determinations. Phys Earth Planet Inter 210:36–49
Zhao LS, Helmberger DV (1994) Source estimation from broadband regional seismograms. Bull Seismol Soc Am 84(1):91–104
Zhu L, Helmberger DV (1996) Advancement in source estimation techniques using broadband regional seismograms. Bull Seismol Soc Am 86(5):1634–1641
Zhu L, Akyol N, Mitchell BJ, Sozbilir H (2006) Seismotectonics of western Turkey from high resolution earthquake relocations and moment tensor determinations. Geophys Res Lett 33(7)
Zoback ML (1992) First- and second-order patterns of stress in the lithosphere: the world stress map project. J Geophys Res 97:11703–11728

Data and Sharing Resources

http://www.globalcmt.org/CMTsearch.html
http://rcmt2.bo.ingv.it/
http://cnt.rm.ingv.it/tdmt